JMEPEG (1997) 6:454-460

Effects of Ion Irradiation on Fatigue of Fe-12Cr-20Mn Stainless Steel for Fusion Reactor Applications

R. Tulluri and D.J. Morrison

To minimize waste disposal problems associated with the residual radioactivity of the first wall material of a fusion reactor, fast induced radioactive decay (FIRD) alloys based on the Fe-Cr-Mn system are being investigated. The objective of this research was to evaluate the effects of irradiation on cyclic strain localization and fatigue crack initiation in a FIRD Fe-12Cr-20Mn alloy and to compare the response to commercially available 316 stainless steel. The alloys were irradiated with 200 keV Fe ions to a dose of 1×10^{16} ions/cm^2 and 15.5 keV He ions to a dose of 7×10^{15} ions/cm^2 to simulate the irradiation-induced defect structure and helium concentration that would be produced in a fusion reactor. Irradiated specimens were fatigued in a cantilever beam fatigue testing machine with the deflection set to produce a fully reversed total strain amplitude of 0.25% on the surface of the specimen. Acetate replicas were obtained during the fatigue tests to provide a record of surface fatigue damage. Transmission electron microscopy (TEM) analyses were performed to characterize the microstructural changes resulting from the irradiations and interactions between fatigue-induced glide dislocations and the irradiation-induced defects.

Results indicate that the irradiated Fe-Cr-Mn alloy exhibits fatigue properties similar to 316 stainless steel. Glide dislocations produced by fatigue cycling annihilate irradiation-induced defects. The defect annihilation causes the formation of cleared channels in which the cyclic plastic strain is localized. Subsurface slip bands penetrate the irradiated regions through the cleared channels and serve as fatigue crack initiation sites.

Keywords fatigue, fusion reactor, radiation effects, stainless steel

1. Introduction

Global energy consumption is increasing at a rate of about 2% per year (Ref 1). At this rate, energy demand will increase by a factor of three by the middle of the next century. To match this increasing rate of energy consumption and to reduce dependence on diminishing fossil fuel resources, there is an urgent need to develop new sources of energy. Nuclear fusion power appears to be a promising energy option for the future. The primary by-product of the fusion reaction is helium, which is both nontoxic and nonradioactive. As a result, the reaction is more environmentally acceptable than nuclear fission. The essentially inexhaustible supply of fusion reaction fuel, namely deuterium and tritium, adds to the above advantages.

There are many problems that must be solved before a commercial scale nuclear fusion reactor can be built and safely operated. The 14 MeV neutrons produced during the reaction will induce radioactivity in the elements that constitute the structural material of the first wall that confines the fusion reaction. This problem is very important in terms of environmental pollution, as the radioactive structural material can no longer be simply recycled or disposed of as nonradioactive waste when the reactor is decommissioned. The solution to this problem lies in choosing materials that exhibit rapid decay of the induced radioactivity, thus minimizing long-term radioactive material disposal problems. High-activation metals such as molybdenum, niobium, tin, cobalt, nickel, and copper take approximately 1000 years for radioactivity to reduce to safe levels, while lower-activation metals such as manganese, vanadium, iron, tantalum, and tungsten take approximately 100 years. A detailed review of the induced radioactivity decay characteristics and biological hazard potentials of many candidate fusion reactor materials was presented by Conn, et al. (Ref 2). The first wall material, therefore, should contain minimum amounts of the elements that do not show a rapid decay of the induced radioactivity. Materials that are developed with this restriction are called fast induced radioactive decay (FIRD) materials. These materials decay to safer levels of radioactivity in a shorter period of time than the high-activation materials. Restrictions on molybdenum and nickel are especially significant because these are primary alloying elements in steels that are currently used in fission reactors. Therefore, to meet the environmental design objective of rapid decay of induced radioactivity, new reactor alloys must be developed.

Extensive work was carried out on austenitic stainless steels for use as the first wall. Austenitic stainless steels have good corrosion resistance, strength, toughness, and ductility at both low and high temperatures. Among austenitic steels, type 316 is a candidate structural material because of the vast experience using this steel in fission reactor applications. However, 316 stainless steel is not a FIRD material because of its high nickel content. One method that can be used to produce a FIRD austenitic stainless steel is to replace nickel with manganese (Ref 3-9). Klueh and Maziasz (Ref 3, 10) studied Fe-Cr-Mn alloys and concluded that an alloy of 12 wt% Cr, 20 wt% Mn, 0.25 wt% C, and balance Fe would possess the desired degree of austenite stability and would exhibit similar or superior mechanical properties to 316 stainless steel.

Design studies have demonstrated that the lifetime of the first wall will be limited by low cycle thermal fatigue. Hardening and loss of ductility as a result of irradiations were previously shown to affect the fracture toughness properties of austenitic steels. In addition, helium can affect the fatigue

R. Tulluri and **D.J. Morrison,** Clarkson University, Potsdam, NY 13699-5725.

properties by contributing to hardening and embrittlement, promoting premature crack initiation, and accelerating crack propagation (Ref 11). Therefore, the objective of this paper is to evaluate the fatigue characteristics of an irradiated FIRD Fe-Cr-Mn steel and to compare these characteristics with those of 316 stainless steel.

2. Experimental Procedures

A vacuum induction melting process was used to produce an ingot with composition 12.12 wt% Cr, 20.16 wt% Mn, 0.23 wt% C, 0.29 wt% Si, and balance Fe. The ingot was hot rolled to a thickness of 2.54 mm and then cold rolled to a thickness of 1.27 mm. AISI 316 stainless steel sheet with composition 17 wt% Cr, 12 wt% Ni, 2 wt% C, 2 wt% Al, 2 wt% Mo, and balance Fe was purchased commercially. Tapered cantilever beam fatigue specimens similar to those used by Eldridge and Morrison (Ref 12) were fabricated from these steels. The specimen geometry, shown in Fig. 1, was designed to produce a constant stress throughout the surface of the tapered gage section. The specimens were annealed at 1100 °C for 45 min and water quenched. They were then mechanically ground to a thickness of 1 mm using SiC abrasive paper and then electropolished in a solution of 350 mL ethanol, 60 mL distilled water, 50 mL butoxyethanol, and 40 mL perchloric acid at a temperature of −30 °C and a potential of 40 V.

Ion irradiations were used to produce the crystal lattice defect structure and helium concentration that would be expected to be produced in the first wall material by the fusion reaction. The specimens were irradiated with 15.5 keV He ions to a dose of 7×10^{15} ions/cm^2 to inject helium into the metal and 200 keV Fe ions to a dose of 1×10^{16} ions/cm^2 to produce irradiation-induced lattice defects. Only the top surface was irradiated. On some specimens, half the gage section was masked so that only the unmasked portion received the ion irradiations.

The advantage of using ion irradiations to simulate the fusion reactor radiation environment is that specimens can be produced much more rapidly and inexpensively than using neutron irradiation. In addition, at the ion energies used in this study, the specimens do not become radioactive. The primary disadvantage of using ion irradiation, especially in studies that address mechanical behavior, is that the ions penetrate only a very shallow distance into the metal. Therefore, only a very thin layer of the surface is irradiated; whereas, neutron irradiation penetrates throughout the bulk of the material.

The relative advantages and disadvantages of using ion beam techniques to simulate the effects of neutron irradiation were discussed in detail by Mazey (Ref 13), and guidelines for using this method are provided in ASTM E 521. Before a material can be certified for use in reactor applications, the material must be tested in an environment that more closely duplicates the temperature and radiation conditions of the reactor. Nonetheless, the room temperature fatigue experiments on ion irradiated specimens reported in the present work provide a simple, inexpensive method to make an initial estimate of the effects of irradiation on material behavior.

Irradiation simulations using the transport of ions in matter (TRIM) program (Ref 13) indicated that the irradiations produced a peak displacements per atom (dpa) of 81 at a depth of 50 nm and a peak helium concentration of 0.76% at a depth of 80 nm. Conventional fatigue studies commonly rely on a cycles-to-failure measurement to evaluate fatigue performance. In this study, the comparison is based on a highly microscopic view of the response of the thin near-surface region to fatigue cycling. Because only a very small part of each specimen was irradiated, a cycles-to-failure result has no relevance in comparing the effects of irradiation on fatigue performance, although the number of cycles to failure provides valuable information concerning the bulk fatigue characteristics of the alloys in the unirradiated condition.

Fatigue experiments on both the irradiated and unirradiated specimens were accomplished at a cycling rate of 25 Hz. The deflection of the fatigue machine was set to produce a fully reversed total strain amplitude of 0.25% at the surface of the gage section. Cycling continued until the formation of fatigue cracks caused the bending moment to drop to 95% of its value at the beginning of the test. Acetate replicas were obtained from the surface of the gage section at regular intervals to study the evolution of the fatigue surface features.

Surface analysis of the effects of fatigue on both irradiated and unirradiated specimens was carried out using optical microscopy. Transmission electron microscopy (TEM) using a JEOL JEM 1200 EX electron microscope (JEOL USA, Inc.,

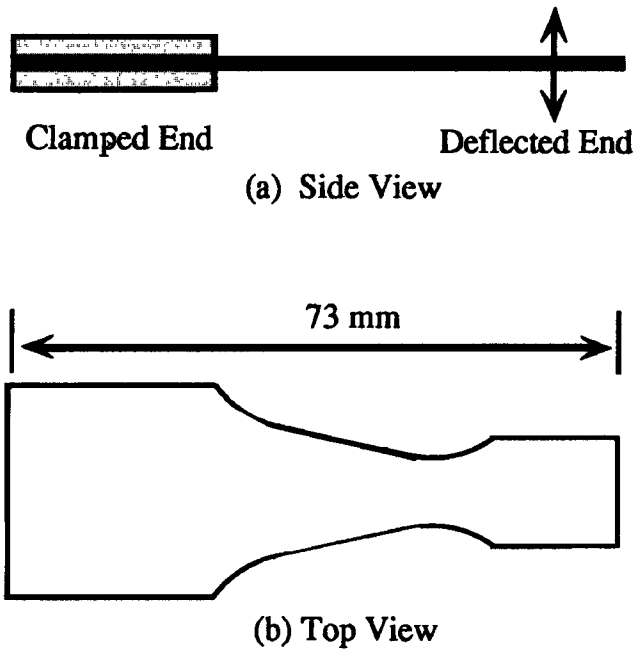

Fig. 1 Cantilever beam fatigue specimen geometry

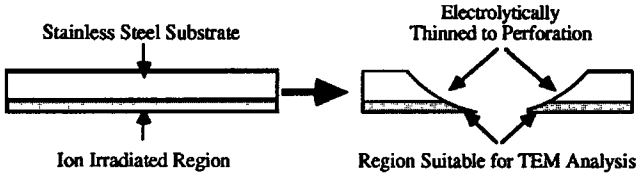

Fig. 2 Schematic representation of the back-thinning process for TEM specimen preparation

Peabody, MA) was performed to analyze the irradiation-induced defect structure and the effects of irradiations on fatigue-induced dislocation structures. To analyze the near-surface defect structure of the specimens, TEM specimens were prepared using the back-thinning technique shown schematically in Fig. 2. In this method, the fatigue characteristics of the thin ion-irradiated regions were analyzed. Electrolytic thinning of the TEM specimens was carried out using a solution of 39 mL perchloric acid, 390 mL methanol, and 221 mL butoxyethanol at 0 °C and a potential of 150 V.

3. Results

3.1 *Microstructural Characterization of the Irradiation-Induced Defects*

TEM micrographs shown in Fig. 3 and 4 depict the near-surface defect structure typically found in the irradiated Fe-Cr-Mn and 316 alloys, respectively, The contrast in these micrographs is caused by the irradiation-induced lattice defects. Similar lattice defect structures were reported by Robinson and Jenkins

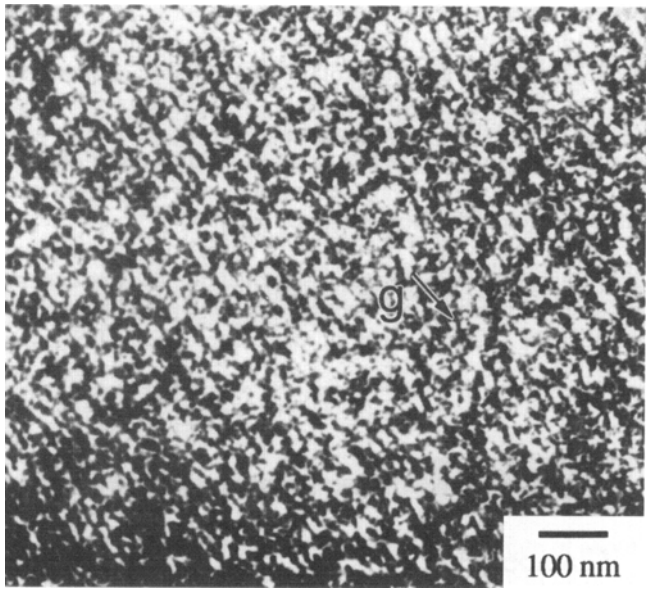

Fig. 3 TEM micrograph showing the irradiation-induced defect structure in the Fe-Cr-Mn alloy. Diffraction vector g = 111 (shown with arrow)

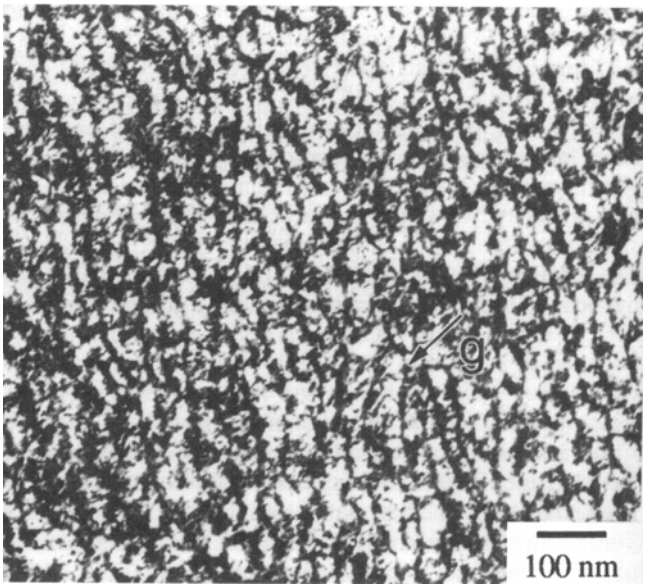

Fig. 4 TEM micrograph showing the irradiation-induced defect structure in the 316 stainless steel alloy. Diffraction vector g = 111

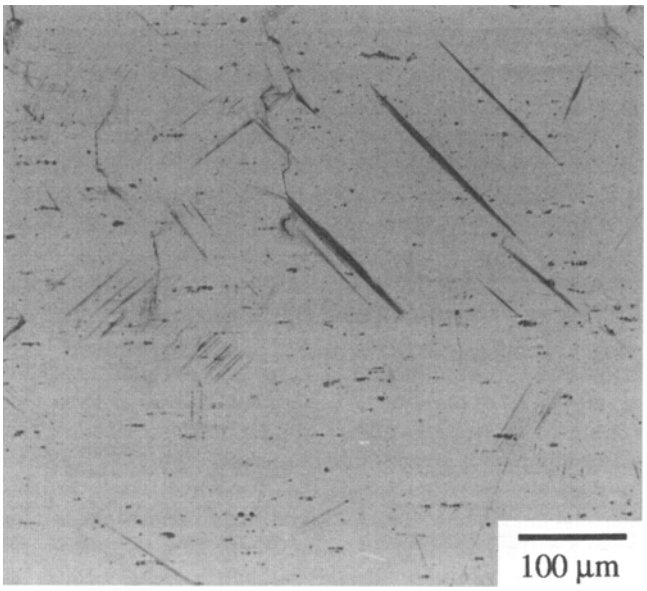

Fig. 5 Optical micrograph of the irradiated and fatigued Fe-Cr-Mn alloy. The upper half was masked during ion irradiation.

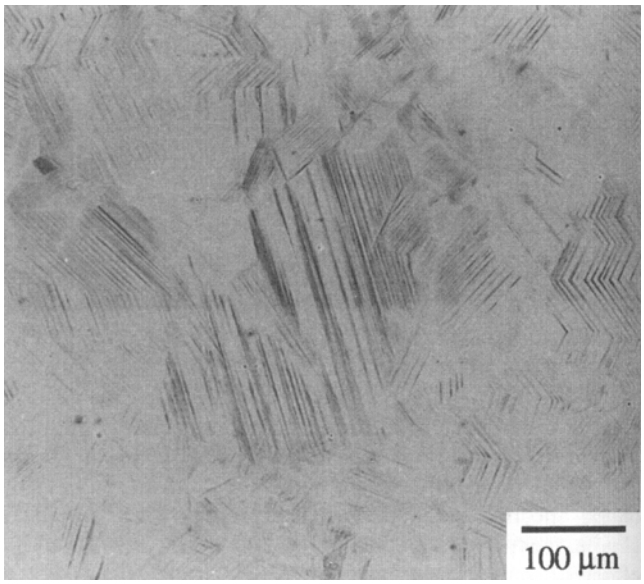

Fig. 6 Optical micrograph of the irradiated and fatigued 316 stainless steel alloy. The upper half was masked during ion irradiation.

(Ref 15) in their work on self-irradiated nickel and nickel alloys. They concluded that the defects were vacancy and interstitial dislocation loops. Clearly the irradiation-induced defect structures produced in the Fe-Cr-Mn and 316 alloys appear very similar. Electron diffraction patterns obtained from these specimens indicated that the irradiated region remained crystalline.

3.2 *Surface Optical Microscopy of the Irradiated and Fatigued Specimens*

Figure 5 shows an optical micrograph of the surface of the irradiated and fatigued Fe-Cr-Mn steel. The specimen was fatigued to 178,000 cycles, which represented the time when the bending moment decreased to 95% of the value at the beginning of the test as a result of the formation of fatigue cracks. The upper half of the micrograph represents the unirradiated region of the specimen, while the lower half represents the irradiated region. The thin parallel bands in the micrograph represent the slip band structure. A clear difference in the surface features between the irradiated and unirradiated regions can be observed in the micrograph. The slip bands were more numerous in the unirradiated region. In addition, the slip bands in the irradiated region were found to be fainter than those in the unirradiated region. From these observations, it can be concluded that the irradiated near-surface region slightly impedes the emergence of slip bands at the surface. However, both irradiated and unirradiated regions showed cracks on the surface. No distinction in number, length, and intensity of cracks was observed between the two regions.

Figure 6 provides an optical micrograph of the surface of the irradiated and fatigued 316 stainless steel. The specimen was fatigued to 175,000 cycles. The upper half of the micrograph shows the unirradiated region, while the lower half shows the irradiated region. While not as pronounced as in the Fe-Cr-Mn specimen, irradiation of the 316 steel caused a slight reduction in the intensity of the surface slip features. However, the number of slip bands appeared to be the same in the two regions. Therefore, it can be concluded that the irradiation has only a slight effect on the emergence of slip bands at the surface in the 316 steel. No distinction in the number, length, and intensity of cracks between the irradiated and unirradiated regions was observed.

3.3 *TEM Analysis of Fatigued Unirradiated Specimens*

The TEM micrograph in Fig. 7 depicts the near-surface region of the unirradiated Fe-Cr-Mn alloy after 180,000 fatigue cycles. The parallel straight bands in the micrograph are slip bands produced during fatigue. The slip bands appeared to run

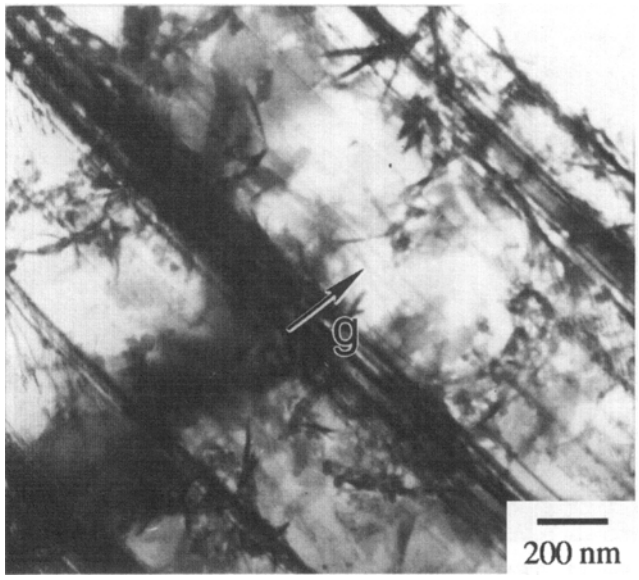

Fig. 7 TEM micrograph of the unirradiated and fatigued Fe-Cr-Mn specimen. Diffraction vector g = 131

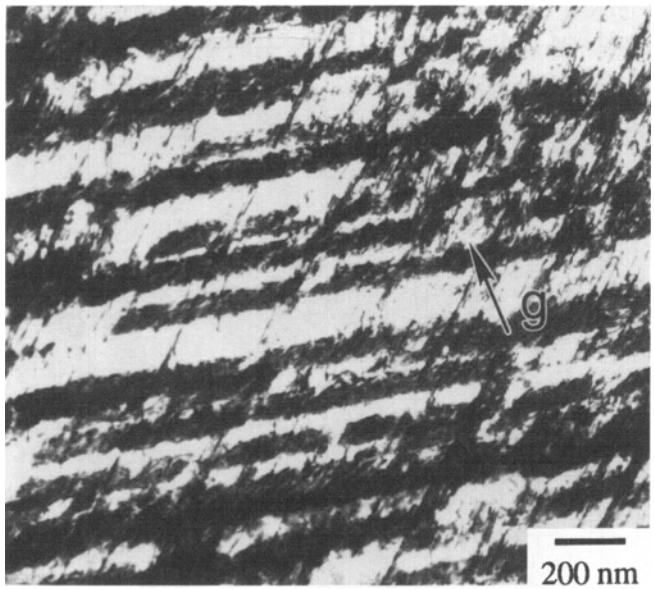

Fig. 8 TEM micrograph of the unirradiated and fatigued 316 stainless steel specimen. Diffraction vector g = 111

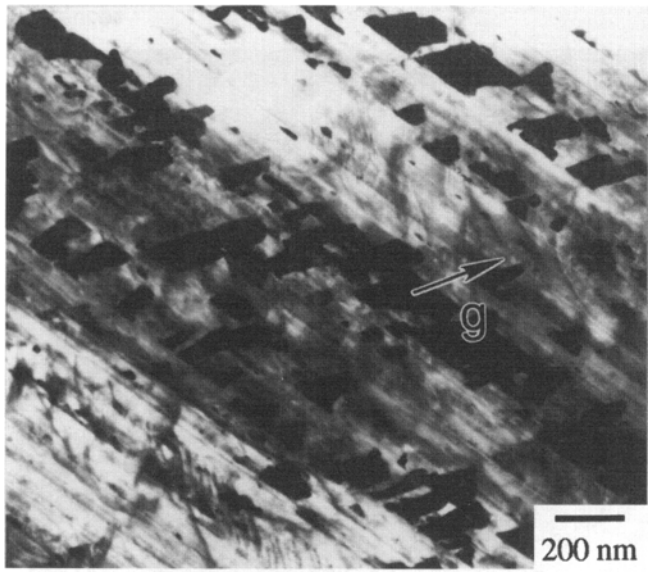

Fig. 9 TEM micrograph of the unirradiated and fatigued 316 stainless steel specimen showing the dark platelike structure. Diffraction vector g = 111

through the entire grain. A less dense dislocation structure was observed between the bands.

Figure 8 shows the dislocation structure in the fatigued 316 stainless steel specimen. The micrograph shows clusters of dislocations formed along parallel slip bands. Slip bands on two different slip systems are shown in the micrograph. In some grains, distinct platelike structures were observed along the slip bands as shown in Fig. 9. The formation of these platelets is believed to be caused by a strain-induced phase transformation.

3.4 *TEM Analysis of Fatigued Irradiated Specimens*

Figure 10 shows a TEM micrograph of the irradiated and fatigued Fe-Cr-Mn specimen. The dark regions between the light bands represent the irradiation-induced defect structure. This structure appears to be similar to that observed in the near-surface region of the unfatigued irradiated Fe-Cr-Mn specimen (Fig. 3). The light parallel bands are dislocation-free channels resulting from the annihilation of the irradiation-induced defects by the moving glide dislocations produced during fatigue. Studies by Greenfield and Wilsdorf (Ref 16) on plastic deformation of neutron-irradiated copper single crystals revealed that interactions between the glide dislocations and irradiation-induced dislocation loops resulted in the annihilation of the dislocation loops. Similar defect-free channels were previously observed in other plastically deformed irradiated metals (Ref 17-20).

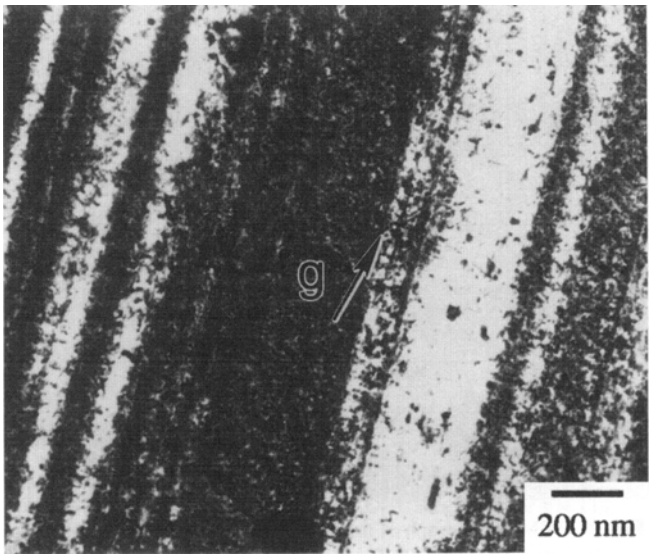

Fig. 10 TEM micrograph of the irradiated and fatigued Fe-Cr-Mn specimen. Diffraction vector g = 111

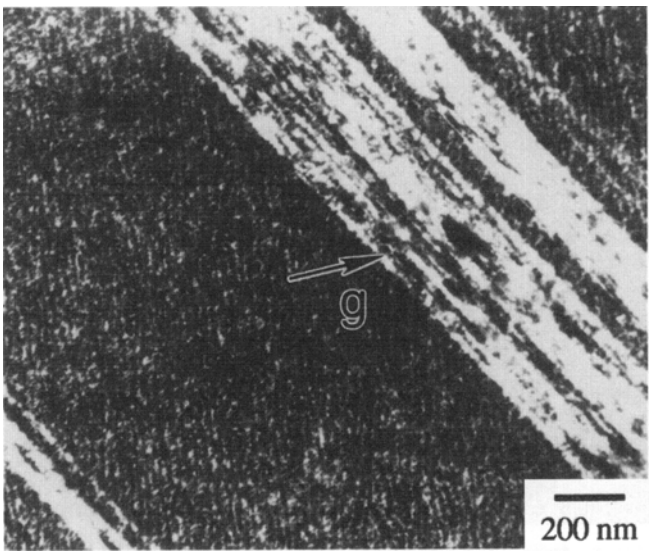

Fig. 11 TEM micrograph of the irradiated and fatigued 316 stainless steel specimen. Diffraction vector g = 200

Figure 11 shows a micrograph of the irradiated and fatigued 316 stainless steel. As was observed in the Fe-Cr-Mn alloy, parallel clear channels resulting from the annihilation of the irradiation-induced defects by the fatigue slip bands were produced. However, as shown in Fig. 12, the channels in the 316 stainless steel showed a dark platelike structure in the bands. These plates are similar to those observed in the unirradiated and fatigued 316 stainless steel shown in Fig. 9. Selected area electron diffraction patterns of the plates indicate that they have the hexagonal close-packed (hcp) crystal structure and are probably ε-martensite.

4. Discussion

Optical microscopy revealed that the 316 steel exhibited only a subtle difference in the surface slip features between irradiated and unirradiated regions, but the Fe-Cr-Mn steel showed a more pronounced difference. The irradiation-induced defects cause a hardening of the irradiated region, which suppresses the emergence of slip bands at the surface. These optical observations appear to be consistent with the TEM results obtained on the irradiated and fatigued specimens. In both

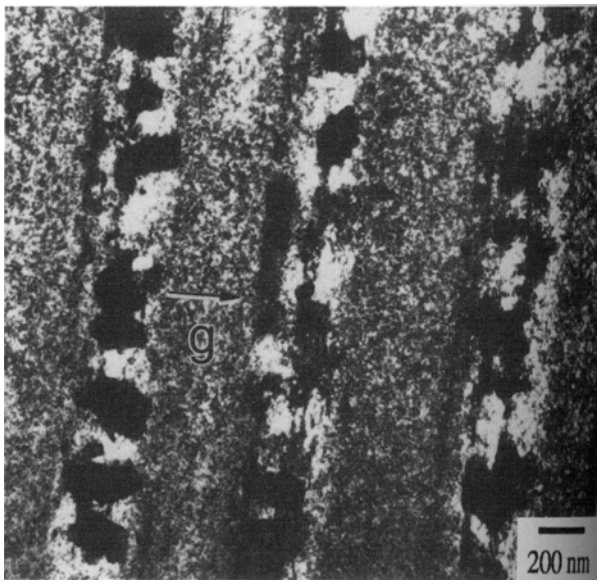

Fig. 12 TEM micrograph of the irradiated and fatigued 316 stainless steel specimen showing the dark platelike structure. Diffraction vector g = 111

alloys, glide dislocations produced by fatigue interact with the irradiation-induced defects to cause localized cyclic softening that results in the formation of clear channels in which plastic strain is concentrated. In this way, subsurface slip bands penetrate the irradiated near-surface region and emerge at the surface. Correlations between surface slip features and subsurface clear channels were reported in other studies (Ref 16-19). Based on the observation that slip band emergence at the surface is more highly suppressed in the Fe-Cr-Mn alloy, it appears that the irradiation-induced defect structure is slightly more stable in this alloy because glide dislocations do not interact as readily with and annihilate the irradiation-induced defects.

The high energy neutrons in a fusion reactor penetrate completely through the first wall material. As a result, the entire volume of the first wall is expected to contain the irradiation-induced defect structure. These defects act as obstacles against dislocation movement during fatigue cycling. Based on the results of the ion-irradiated Fe-Cr-Mn and 316 alloys presented in this study, it would be expected that in neutron-irradiated specimens, the glide dislocations will form clear channels by locally annihilating the irradiation-induced defect structure. However, these channels will form more easily in the 316 stainless steel. The effect that the formation of clear channels has on fatigue life depends on whether the channels cause enhanced strain localization. If the channels localize the plastic strain in a fewer number of slip bands, irradiation will decrease the fatigue life. However, it is possible that strain may be homogeneously distributed by the formation of a very large number of channels. For example, in the 316 alloy, channels appear to form very easily. As a result, irradiation would not be expected to significantly affect the fatigue life because plastic strain is distributed over many slip bands. Conversely, in alloys in which channel formation is more difficult, the plastic strain may be localized along fewer slip bands. The greater degree of strain localization would be expected to decrease the fatigue life. In the extreme case of materials that do not form channels, the fatigue life would actually be increased because plastic deformation is essentially eliminated as a result of the irradiation hardening and increase in yield strength. However, in this case, embrittlement would be more of a concern, and crack propagation would be quite rapid. From the results of this study, irradiation may cause a more pronounced localization of plastic strain in the Fe-Cr-Mn alloy. However, this preliminary study cannot predict the extent of this effect. Indeed, TEM results indicate that clear channels do form in the Fe-Cr-Mn alloy, and the effect may be minor.

Helium bubble formation was not observed in the steels analyzed. This is due to the fact that the irradiations and fatigue experiments were accomplished at room temperature. A temperature above 600 °C is required to provide sufficient diffusion for the helium bubbles to grow to detectable sizes (Ref 21). Future studies will address the elevated temperature irradiation and fatigue characteristics of the materials.

5. Conclusions

The following conclusions can be drawn from the results obtained in this work:

- In the unirradiated condition, the Fe-Cr-Mn and 316 alloys exhibited similar fatigue properties as measured by the number of cycles for the bending moment to diminish to 95% of the initial value.
- The effects of irradiation defects on the microstructure of the Fe-Cr-Mn and 316 stainless steels were similar. Both steels showed defect structures in the forms of vacancy and interstitial dislocation loops.
- Both alloys showed a similar interaction of the cyclic dislocation structure with the irradiation-induced defects. The moving glide dislocations produced by fatigue locally annihilated the irradiation-induced defects and resulted in the formation of the dislocation-free channels. As a result, the resistance against further glide dislocation movement was reduced, and the clear channels emerged at the surface as slip bands. Clear channels appeared to form more easily in the 316 alloy. The effect that the formation of clear channels has on fatigue life depends on whether the channels cause enhanced strain localization. Therefore, it is possible that the effect may be very sensitive to the magnitude of the fatigue load or strain amplitude.
- The FIRD Fe-Cr-Mn austenitic stainless steel appears to be a promising substitute for 316 austenitic stainless steel for use as the first wall material in a fusion reactor.

These results demonstrate that more detailed studies that include thermal effects and a more realistic irradiation exposure are warranted.

Acknowledgments

This research was sponsored by the National Science Foundation under grant 9108695. Ion irradiations were accomplished at the Michigan Ion Beam Laboratory for Surface Modification and Analysis. The assistance of Dr. Victor Rotberg is gratefully acknowledged.

References

1. R.S. Pease, Global Energy Scenarios and the Potential Role of Fusion Energy in the 21st Century, *J. Nucl. Mater.*, Vol 191-194, 1992, p 7-14
2. R.W. Conn, E.E. Bloom, J.W. Davis, R.E. Gold, R. Little, K.R. Schultz, D.L. Smith, and F.W. Wiffen, Lower Activation Materials and Magnetic Fusion Reactors, *Nucl. Technol./Fusion,* Vol 5, 1994, p 291-310
3. R.L. Klueh and P.J. Maziasz, Reduced Activation Austenitic Stainless Steels: The Fe-Mn-Cr-C System, *Reduced Activation Materials for Fusion Reactors—ASTM STP 1047,* R.L. Klueh, D.S. Gelles, M. Okada, and N.H. Packan, Ed., ASTM, 1990, p 7-18
4. H. Yoshida, K. Miyata, H. Kodaka, and S. Nishikawa, Irradiation Effects on Mechanical Properties of High Manganese Steels, *Reduced Activation Materials for Fusion Reactors—ASTM STP 1047,* R.L. Klueh, D.S. Gelles, M. Okada, and N.H. Packan, Ed., ASTM, 1990, p 47-55
5. P. Fenici and H. Scheurer, Tensile Properties of Neutron Irradiated Cr-Mn Austenitic Stainless Steels, *J. Nucl. Mater.*, Vol 155-157, 1988, p 947-952
6. F.A. Garner, F. Abe, and T. Noda, Response of Fe-Cr-Mn Austenitic Alloys to Thermal Aging and Neutron Irradiation, *J. Nucl. Mater.*, Vol 155-157, 1988, p 870-876

7. J.M. McCarthy and F.A. Garner, Phase Instabilities in Irradiated Simple Fe-Cr-Mn Low Activation Alloys, *J. Nucl. Mater.,* Vol 155-157, 1988, p 877-882
8. K. Miyahara, Y. Okazaki, M. Mochizuki, Y. Hosoi, and H. Kayano, Mechanical Properties and Microstructure of α-Particle Irradiated Fe-12%Cr-15.30%Mn Alloys, *J. Nucl. Mater.,* Vol 155-157, 1988, p 1054-1058
9. A.V. Vertkov, V.A. Evtikhin, I.E. Lyublinski, A.A. Syichev, E.V. Demina, and M.D. Prusakova, Mechanical Properties of Low-Activation Cr-Mn Austenitic Steels Changes in Liquid Lithium, *J. Nucl. Mater.,* Vol 203, 1993, p 158-163
10. P.J. Maziasz and R.L. Klueh, Precipitation Sensitivity to Alloy Composition in Fe-Cr-Mn Austenitic Steels Developed for Reduced Activation for Fusion Application, *Reduced Activation Materials for Fusion Reactors—ASTM STP 1047,* R.L. Klueh, D.S. Gelles, M. Okada, and N.H. Packan, Ed., ASTM, 1990, p 56-79
11. H. Trinkaus and H. Ullmaier, The Effect of Helium on the Fatigue Properties of Structural Materials, *J. Nucl. Mater.,* Vol 155-157, 1988, p 148-155
12. I. Eldridge and D.J. Morrison, Microstructures and Mechanical Properties of Welded Fe-12Cr-20Mn Austenitic Stainless Steel, *J. Mater. Eng. Perform.,* Vol 3, 1994, p 606-611
13. D.J. Mazey, Fundamental Aspects of High-Energy Ion-Beam Simulation Techniques and Their Relevance to Fusion Materials Studies, *J. Nucl. Mater.,* Vol 174, 1990, p 196-209
14. J.F. Ziegler, J.P. Biersack, and U. Littmark, *The Stopping and Range of Ions in Solids,* Pergamon, 1984
15. T.M. Robinson and M.L. Jenkins, Heavy Ion Irradiation of Nickel and Nickel Alloys, *Philos. Mag. A,* Vol 43, 1981, p 999-1015
16. I.G. Greenfield and H.G.F. Wilsdorf, Effect of Neutron Irradiation on the Plastic Deformation of Copper Single Crystals, *J. Appl. Phys.,* Vol 32, 1961, p 827-839
17. J.J. Wang, G.E. Welsch, H. Bakhru, A. Mashayekhi, and W. Gibson, TEM Evaluation of Ion Implanted and Fatigued Metal Surface Layers, *Nucl. Instrum. Methods B,* Vol 7-8, 1985, p 228-234, 1985
18. J.V. Sharp, Deformation of Neutron-Irradiated Copper Single Crystals, *Philos. Mag.,* Vol 16, 1967, p 77-96
19. J.V. Sharp, Correlation Between Cleared Channels and Surface Slip Steps in Neutron Irradiated Copper Crystals, *Radiat. Eff.,* Vol 14, 1972, p 71-75
20. D.J. Morrison, J.W. Jones, D.E. Alexander, and G.S. Was, Influence of Cyclic Deformation on Surface Microstructure and Hardness of Ion-Implanted Nickel, *Metall. Trans. A,* Vol 22, 1991, p 1633-1645
21. P. Fenici, Influence of Light Ion Irradiation on Fatigue Crack Propagation in Austenitic Stainless Steel, *J. Nucl. Mater.,* Vol 155-157, 1988, p 963-967